10-14-2020

Case Study: Unsaturated Embankment Failure on Soft Soils

Ghada Ellithy
Embry-Riddle Aeronautical University, Ghada.Ellithy@erau.edu

Timothy D. Stark
University of Illinois

Case Study: Unsaturated Embankment Failure on Soft Soils

Ghada S. Ellithy, Ph.D., P.E., M.ASCE[1]; and Timothy D. Stark, Ph.D., P.E., D.GE, F.ASCE[2]

Abstract: This paper describes the application of unsaturated soil mechanics to an interstate connecting-ramp embankment that failed during construction. Specifically, matric suction is incorporated into the calculation of the tension crack (TC) depth induced by desiccation and strain incompatibility and the contribution of matric suction to embankment shear strength. The results are compared with field observations to assess the viability of unsaturated soil mechanics in modeling compacted embankments in stability analyses. Results from this study suggest that using unsaturated shear strength parameters while introducing a TC in the compacted fill yields a reasonable inverse analysis of this interstate embankment. This may be preferred in slope stability analyses to the current practice of using an undrained shear strength (i.e., cohesion) for the unsaturated compacted fill and including a TC to generate a reasonable factor of safety. **DOI: 10.1061/(ASCE)GT.1943-5606.0002382.**

Author keywords: Unsaturated soil; Inverse analysis; Shear strength; Suction; Slope stability; Compacted fill; Desiccation; Strain incompatibility; Tension crack.

Introduction

Employing unsaturated soil mechanics can provide a rational basis to explain the service state behavior of compacted embankments as well as a platform for performing inverse analyses of slopes, foundations, and earthen structures. The majority of foundation soils, earthen structures, and compacted slopes are comprised of unsaturated soils or they at least experience unsaturated conditions during their life span. Presence of negative pore water pressure, or suction, in the unsaturated zone can affect key engineering attributes of the soil, such as shear strength and compressibility. The extent of this effect depends on several factors including soil type and hydro-mechanical properties of the soil, which can be significant in fine-grained soils.

In design, the contribution of suction is legitimately ignored, primarily due to uncertainties associated with its longevity during the structure service life. In addition, the suction contribution can quickly degrade and possibly vanish upon wetting (Stark and Duncan 1991). However, understanding and incorporating the variation of suction into analyses of unsaturated slopes and earthen structures can accurately interpret field-measured data for inverse analysis purposes, such as studying the effect of desiccation and surface vegetation.

Most of the slope instability related research in unsaturated soils deals with the effect of rain infiltration into natural or compacted slopes (Ng and Shi 1998; Gasmo et al. 2000; Oh and Vanapalli 2010; Oh and Lu 2015). For example, Oh and Vanapalli (2010) performed stability analyses of a homogeneous compacted unsaturated embankment constructed using glacial till. They analyzed long- and short-term conditions using saturated and unsaturated conditions. They concluded that the critical stability condition arises when rainfall infiltrates into an unsaturated embankment, however, they do not include a tension crack in the slope, as subsequently discussed.

Oh and Lu (2015) present two case studies of failed cut slopes due to rainfall in Korea. They concluded that an unsaturated hydro-mechanical framework accurately predicts the failures under transient rainfall conditions. They state that incorporating unsaturated effective stress principles in slope stability analysis yield less conservative designs than traditional total stress methods. Similar to the work by Oh and Vanapalli (2010), there was no tension cracking involved in the two slopes analyzed.

Lau (1987) states that desiccation cracks initiate at a matric suction of less than 10 kPa for silty and clayey soils based on laboratory testing. He presented two expressions for predicting desiccation crack depth based on volume change (elastic equilibrium) and shear strength (plastic equilibrium). He stated that the elastic equilibrium analysis provides a better prediction of desiccation crack depth and is based on depth to groundwater and elastic modulus as a function of total and effective stresses.

Michalowski (2014) presents slope stability method with a tension crack based on a kinematic approach (plastic deformation). He concluded that crack formation is an important factor affecting the outcome of stability analyses of slopes but he did not include the effect of the matric suction.

Case Study

In this case study paper, unsaturated soil mechanics principles are used to investigate the failure of a 91 m (300 ft) long section of an interstate connecting-ramp embankment (Ramp ES) between westbound Interstate-76 (I-76) to southbound Interstate 71 (I71) in Medina County, Ohio. After placement of only 2.4 m (8 ft) of the embankment fill, or just over one-quarter of the long-term embankment height of 9.2 m (30 ft) at this location, tension cracks

[1]Senior Research Geotechnical Engineer, US Army Corps of Engineers, Engineering Research and Development Center, 3909 Halls Ferry Rd., Vicksburg, MS 39180. Email: Ghada.S.Ellithy@usace.army.mil

[2]Professor, Dept. of Civil and Environmental Engineering, Univ. of Illinois at Urbana–Champaign, 205 N. Mathews Ave., Urbana, IL 61801 (corresponding author). ORCID: https://orcid.org/0000-0003-2384-1868. Email: tstark@Illinois.edu

Note. This manuscript was submitted on June 5, 2019; approved on June 18, 2020No Epub Date. Discussion period open until 0, 0; separate discussions must be submitted for individual papers. This paper is part of the ***Journal of Geotechnical and Geoenvironmental Engineering***, © ASCE, ISSN 1090-0241.

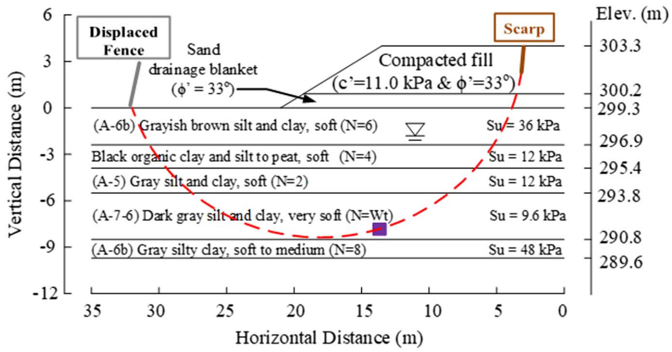

Fig. 1. Subsurface cross section for the failed embankment and estimated undrained shear strengths based on Boring ES-8C at Station 203 + 58, depth of shear displacement at 12.5 m (~41 ft) in slope inclinometer at Station 200 + 00 (solid square) at Elevation +291.7 m, and inferred failure surface (dashed line).

(TCs) developed along the crest of the embankment. After the embankment height reached about 43% (4.0 m or 13 ft) of the long-term height (9.2 m or 30 ft), a 91 m (300 ft) long section of the embankment failed in 2007. The maximum embankment height during construction was to be 9.7 m (32 ft) to reflect a 0.6 m (2 ft) surcharge to preload the foundation soils that would be removed before pavement placement. Stark et al. (2018) presented an undrained or saturated inverse analysis of this case history. Interested readers are referred to Stark et al. (2018) for further details regarding the embankment construction and failure, which are not repeated herein.

This paper presents an unsaturated inverse stability analysis that incorporates matric suction of the embankment and TC depth induced by desiccation and strain incompatibility into the analysis. Further, a set of slope stability analyses are performed while accounting for the contribution of matric suction to the embankment shear strength. The results are compared with field observations to assess the viability of unsaturated soil mechanics providing further insight into this embankment failure. Results from this study suggest that using unsaturated shear strength parameters while introducing a TC in the compacted fill yields a reasonable inverse analysis of this interstate embankment failure.

Subsurface Conditions

Fig. 1 shows the embankment cross section close to the center of the failure area at Station 203 + 58. The groundwater level was found after drilling in Boring ES-8C at a depth of about 2 m (6.6 ft). Fig. 1 also shows a failure surface that corresponds to the TCs observed on the embankment crest; the shear displacement in a slope inclinometer at Station 200 + 00, which is 109.2 m (358 ft) away from Station 203 + 58 at a depth of approximately 12.5 m (~41 ft); the observed uplifted toe of the slide mass; and a fence displaced by the slide mass. Table 1 shows the index properties for the foundation soils at Station 206 + 58 based on Boring ES-8C.

Table 1 presents the index properties for the foundation soils at Station 203 + 58 based on Boring ES-8C. The reader should refer to Stark et al. (2018) for further details on the subsurface conditions and soil properties of the embankment and foundation soils at the failure location.

Undrained Strength of Compacted Fill

In the initial design, the embankment was modeled using a total stress or undrained shear strength (i.e., cohesion) even though the compacted soil was unsaturated. Stark et al. (2018) showed that the use of a cohesion and lack of a TC in the unsaturated compacted fill inflated the calculated factor of safety in the initial design. The embankment contribution of shear resistance was about 50% of the total shear resistance mobilized along the failure surface and resulted in the design factor of safety being overestimated by 2.0–2.5 times because an embankment TC was not included in the initial design analysis (Stark et al. 2018).

The compacted fill strength parameters used for the initial design analysis are a total stress cohesion (c) or undrained shear strength of 71.8 kPa (1,500 psf) and a total stress friction angle (ϕ) of zero (Table 2). This is in accordance with Ohio Department of Transportation (ODOT) Geotechnical Bulletin GB-6 (ODOT 2010), which was available at the time of design. GB-6 recommended using values of cohesion of 71.8–95.8 kPa (1,500–2,000 psf) and ϕ of zero for short-term analyses. The calculated FS using a cohesion of 71.8 kPa (1,500 psf) and a fill height of 4.6 m (15 ft) is 1.64, which confirms the original design met ODOT FS requirements, but overpredicted the actual or field FS because the slope failed, that is, FS ~ 1.0, at a fill height of 4.0 m (13 ft) or 43% of the long-term height (9.2 m or 30 ft).

The contract required that the embankment be placed and compacted per Section 203 (Earthwork) of the ODOT Construction and Materials Specifications, which requires under Section 203.06 spreading all embankment material, except for rock, in successive horizontal loose lifts, not to exceed 200 mm (8 in.). In addition, Section 203.07.A requires that the moisture content of embankment materials be adjusted to meet the density requirements under 203.07.B. Under Section 203.07.B, all embankment materials, except for rock, should be compacted in horizontal lifts to a dry density greater than the percentages of maximum dry density based on standard Proctor compactive effort provided in Table 2013.07-1, which is reproduced in Table 3. The embankment was placed with a dry density greater than 1,921 kg/m^3 (120 lbs/ft^3), that is, more than 102% of standard Proctor maximum dry density and the moisture content needed to achieve this density. The unsaturated soil parameters were estimated using a degree of saturation in the range of 80%, which is about the value of target compaction water content around the optimum moisture content.

Table 1. Index properties for foundation soils at Station 203 + 58 based on Boring ES-8C

Visual soil type	ODOT symbol	In situ moisture content (%)	Liquid limit	Plastic limit	Plasticity index	Calculated USCS symbol	Estimated percentage passing no. 200 sieve (%)
Gray/brown silt and clay	(A6-b)	24, 33, 37	52	51	1	MH	>35%
Black organic clay and silt	—	222, 241	N/A	N/A	N/A	N/A	<20%
Gray silt and clay	(A-5)	124, 92	57	49	8	MH	>35%
Dark gray silt and clay	(A-7-6)	49, 45 35	44	23	21	CL	>35%
Gray silty clay	(A-6b)	17, 17	N/A	N/A	N/A	N/A	>35%

Table 2. Slope stability input parameters for subsurface cross section at Station 203 + 58 based on Boring ES-8C

Soil type	Total and saturated unit weights [kN/m^3 (pcf)]	Undrained shear strength or c' [kPa (psf)]	Total (ϕ) stress or effective (ϕ') friction angles (degrees)
Compacted fill	21.2 (135)	71.8 (1,500) or 14.4 (300)	$\phi = 0$ or $\phi' = 33$
Sand drainage blanket	18.6 (120)	0	$\phi' = 33$
(A6-b) gray/brown silt and clay	17.3 (110)	36 (752)	$\phi = 0$
Black organic clay and silt to peat	11.8 (75)	12 (250)	$\phi = 0$
(A-5) gray silt and clay	17.3 (110)	12 (250)	$\phi = 0$
(A-7-6) dark gray silt and clay	15.7 (100)	9.6 (200)	$\phi = 0$
(A-6b) gray silty clay	18.1 (115)	48 (1,000)	$\phi = 0$

Table 3. Embankment compaction requirements

Maximum laboratory dry weight [kg/m^3 (lbs/ft^3)]	Minimum compaction requirements in percent of laboratory maximum.
1,440–1,680 (90–104.9)	102
1,681–1,920 (105–119.9)	100
1,921 and more (120 and more)	98

Undrained Strain Incompatibility

Modeling the compacted fill with an undrained strength or cohesion can overestimate the strength of a compacted fill slope on soft foundation soils unless a TC is included in the analysis. A TC is required because of the strain incompatibility between the stiff embankment and the soft underlying foundation soils. This can result in the percentage of strength mobilized in the embankment being smaller than in the foundation soils (Chirapuntu and Duncan 1976). A TC develops in the embankment usually near the bottom of the embankment and propagates upward due to lateral deformation of the foundation soils.

The depth of the TC, H_{crack}, that should be used in a stability analysis can be estimated assuming a planar failure surface and the following expression derived from Rankine active earth pressure theory (see Peck et al. 1974):

$$H_{crack} = \frac{2 \times c_{fill}}{\gamma_{Fill} * \tan(45° - \frac{\emptyset_{fill}}{2})} \qquad (1)$$

where γ_{fill}, ϕ_{fill}, and c_{fill} = unit weight, total stress friction angle, and total stress cohesion of the compacted fill, respectively.

Using a value of c_{fill} of 71.8 kPa (1,500 psf), and ϕ_{fill} of zero in Eq. (1) results in a TC depth of 6.7 m (22 ft). This TC depth exceeds the height of the highway embankment when TCs started to develop [i.e., 2.4 m (8 ft)] and when the embankment failed at a fill height of only 4.0 m (13 ft). This indicates that no shear resistance should have been used for the embankment in the design stability analyses. However, the use of an undrained shear strength and a TC for an unsaturated compacted embankment stability analysis is troubling for future designs due to the following reasons:

- Compacted fill is unsaturated but it is modeled using an undrained shear strength that corresponds to a saturated soil (i.e., ϕ equal to zero strength condition).
- Shear resistance of the compacted fill changes with depth or confining pressure.
- Shear resistance of the compacted fill changes with matric suction pressure or volumetric moisture content so the embankment strength is not constant with depth and can change with time due to precipitation or other wetting.
- A TC was not visible until the slope movement occurred at a fill height of only 2.4 m (8 ft), so inclusion of a TC in design does not match field observations and is used simply to reduce the impact of using an undrained shear strength.
- Failure cannot be explained without a full-depth TC (i.e., full strain incompatibility).

To address the aforementioned limitations using an undrained shear strength and a TC analysis, this case study paper employs unsaturated soil mechanics to model the compacted embankment. In particular, this paper presents an unsaturated inverse stability analysis that includes the effect of suction pressure on embankment shear strength and a TC depth that accounts for desiccation and strain incompatibility effects. Using unsaturated soil mechanics allows a more rational framework for the inverse analysis instead of tricking the analysis with an undrained shear strength measured using unconfined compression tests on unsaturated specimens.

Unsaturated Shear Strength Modeling

The role of matric suction in the stability of unsaturated slopes can be quantified by its effect on either shear strength or effective stress variations above the groundwater surface. The majority of currently available unsaturated slope stability methods use the independent stress state variable approach proposed by Fredlund et al. (1977), which treats the normal stress and matric suction as independent stress variables to evaluate the shear strength of unsaturated soils. Based on this approach, Fredlund et al. (1978) extend the traditional Mohr-Coulomb shear strength equation to express the unsaturated strength of soil by separating the independent stress state variables of *net total stress* (σ–u_a) and *matric suction* (u_a–u_w) as follows:

$$\tau_f = c' + (\sigma - u_a) \times \tan\phi' + (u_a - u_w) \times \tan\phi^b \qquad (2)$$

where u_a and u_w = pore air and pore water pressures, respectively; σ = applied total stress; ϕ' and c' = effective stress friction angle and cohesion, respectively; and ϕ^b = friction angle defining the increase in shear strength due to matric suction. For a saturated soil, u_a is equal to zero, u_w is positive (compressive), and ϕ^b becomes ϕ', which describes the rate of increase in shear strength with increasing the effective stress so Eq. (2) simplifies to the classical Mohr-Coulomb shear strength equation.

The soil-water characteristic curve (SWCC) describes the constitutive relationship between matric suction (ψ) and volumetric water content of an unsaturated soil (θ). The SWCC is the key soil information required for the analysis of seepage, stability, and volume change problems involving unsaturated soils (Fredlund 2002). Vanapalli et al. (1996) proposed the following expressions for predicting the shear strength of an unsaturated soil, which estimates the $\tan\phi^b$ term in Eq. (2) using the SWCC:

$$\tau_f = c' + (\sigma - u_a)\tan\phi' + (u_a - u_w)[(\Theta)^{\kappa}(\tan\phi')] \qquad (3)$$

or alternatively

$$\tau_f = c' + (\sigma - u_a)\tan\phi' + (u_a - u_w)\left[\left(\frac{\theta - \theta_r}{\theta_s - \theta_r}\right) \times (\tan\phi')\right] \tag{4}$$

where Θ = normalized volumetric water content, which equals the degree of saturation S; κ = a fitting parameter; θ_s = volumetric moisture content at full saturation (equal to porosity); and θ_r = residual volumetric moisture content, which is described in the next subsection. Fitting functions for κ [Eq. (3)], in terms of soil plasticity index (PI), have been developed for clayey soils for suction values up to about 500 kPa (Vanapalli and Fredlund 2000; Garven and Vanapalli 2006).

Comparing Eqs. (2) and (4) yields the following expression for the $\tan\phi^b$ term:

$$\tan\phi^b = \left[\left(\frac{\theta - \theta_r}{\theta_s - \theta_r}\right) \times (\tan\phi')\right] \tag{5}$$

This expression utilizes the ratio of volumetric water contents that can be rewritten as

$$\left(\frac{\theta - \theta_r}{\theta_s - \theta_r}\right) = S_e = \left(\frac{S - S_r}{1 - S_r}\right) \tag{6}$$

where S_e = effective saturation; S = degree of saturation; and S_r = residual saturation.

Vanapalli et al. (1999) introduce a wetting term when determining $\tan\phi^b$ to account for the increase in saturation during undrained loading of an unsaturated soil. Fredlund and Vanapalli (2002) state that during undrained loading, the increase in shear strength caused by the increase in applied stress is greater than the reduction in shear strength associated with the decrease in matric suction (due to an increase in saturation). Fredlund and Rahardjo (1993) state that the change in suction due to the application of a deviator stress is commonly neglected in undrained tests on unsaturated soil. This statement indicates that for undrained loading, either Eq. (3) or Eq. (4) could be used as an approximation of the undrained shear strength.

Similar to saturated soils, the shear strength of unsaturated soil has to be interpreted in terms of total stresses at failure if the pore water pressures are not measured or controlled. The total stress approach for unsaturated soils should be applied in the field only if the strength measured in the laboratory has relevance to the field drainage conditions (Fredlund and Vanapalli 2002). In the lack of such laboratory measurements or an accurate determination of $\tan\phi^b$, the previous approximation can be used with a SWCC and an estimated matric suction to assess stability, as subsequently illustrated. The shear strength contribution due to matric suction, $(u_a - u_w) \times (\tan\phi^b)$, can be estimated assuming a linear strength envelope inclined at ϕ' (Fredlund et al. 2012). This type of analysis is more representative of unsaturated field conditions than using an undrained shear strength (i.e., Su and $\phi = 0$) and introducing a representative TC as done by Stark et al. (2018) in their inverse analysis of this highway embankment.

Use of SWCC to Estimate $\tan\phi^b$

To estimate the $\tan\phi^b$ term in Eqs. (2) and (5), the SWCC must be determined for the investigated soil. While the SWCC can be directly measured, several models have been developed over the last two decades to estimate the SWCC because of their simplicity and accuracy in estimating the SWCC from index properties (Ellithy et al. 2017). These models can be either in the form of a closed-form analytical solution that models experimentally derived SWCCs [e.g., Gardner (1958); Brooks and Corey (1964); van Genuchten (1980); and Fredlund and Xing (1994)] or predictive models correlated to basic soil index properties, such as grain size distribution and Atterberg limits, for an example, Zapata et al. (2000), Aubertin et al. (2003), and Benson et al. (2014).

The van Genuchten (1980) SWCC analytical model is popular and is given by

$$\theta = \theta_r + \frac{\theta_s - \theta_r}{[1 + (\frac{\psi}{a})^n]^m} \tag{7}$$

where ψ = matric suction; a, n, and m = fitting parameters dependent on the air entry value (AEV), rate of soil drainage, pore size characteristics, and the overall shape of SWCC, respectively. The parameter a has the same dimensions as ψ, and m can be estimated as $(1\text{–}1/n)$, in which n and m are dimensionless.

In this study, the shear strength equation based on independent stress state variables [Eq. (2)] along with van Genuchten's SWCC model were used for the inverse analysis of the failed compacted embankment. Ellithy (2017) developed a user-friendly spreadsheet that utilizes different SWCC predictive and analytical models including van Genuchten (1980). Due to the lack of laboratory and field testing of the highway embankment unsaturated soil properties, the method described in Ellithy (2017) was used to estimate the van Genuchten (1980) SWCC fitting parameters and corresponding unsaturated shear strength parameters for the compacted embankment using index properties from the initial subsurface investigation (Table 4).

Table 4. Soil properties for failed compacted embankment

Compacted fill properties	Value
Liquid limit (LL)	33%
Plastic limit (PL)	19%
Plasticity index (PI)	14%
Total unit weight (constant) (γ)	21.2 kN/m^3
Void ratio (e)	0.80
Porosity (p) *or* saturated volumetric moisture content (θ_s)	0.44
Residual volumetric moisture content (θ_r)	0.08
van Genuchten (1980) fitting parameter (a)	47 kPa
van Genuchten (1980) fitting parameter (n)	1.5
Effective stress friction angle (ϕ')	33°
Effective stress cohesion (c')	14.4 kPa
Saturated hydraulic conductivity (k_{sat})	1.0×10^{-6} cm/s

TC Depths

In an unsaturated stability analysis involving a stiff compacted embankment constructed over soft foundation soils, two types of TCs can develop and must be incorporated in the analysis to reflect the unsaturated behavior of the compacted embankment. These two TCs are due to (1) desiccation at the embankment surface, and (2) strain incompatibility between the stiff compacted embankment and underlying soft foundation soils, which starts from the bottom of the embankment and propagates upward. The first subsection focuses on estimating the depth of the TC due to desiccation at the top of the compacted embankment, and the subsequent subsection addresses the TC from the bottom of the embankment due to strain incompatibility with the foundation soils.

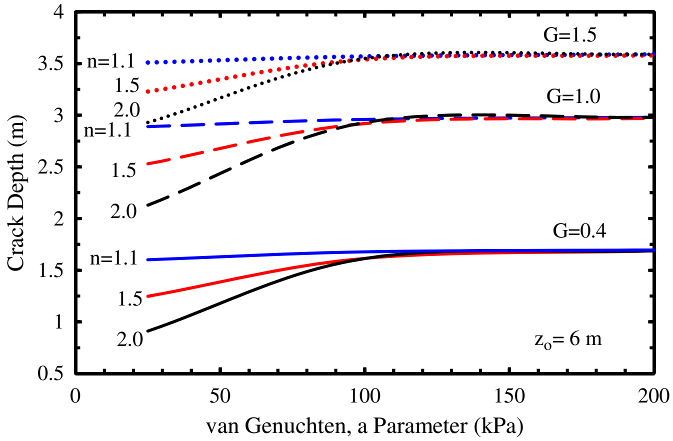

Fig. 2. Sensitivity of steady-state desiccation tension crack depth to van Genuchten (1980) parameters a and n for a groundwater depth (z_o) of 6 m.

Desiccation TC Depth

Because soil has a relatively low shear resistance in tension, desiccation cracking may develop when the value of the coefficient of earth pressure at rest, K_0, approaches zero. Desiccation cracking occurs in unsaturated soils and is not associated with slope instability. Lu and Likos (2004) demonstrate that the TC depth under a steady-state hydrostatic condition (i.e., the specific discharge equals zero or no infiltration or evaporation exists through the unsaturated soil mass) can be estimated using the following expression:

$$Z_o - Z = G\frac{Z}{(1+Z^n)^{(n-1)/n}} \quad (8)$$

where $Z_o = \gamma_w z_o/a$; z_o = depth to groundwater; γ_w = unit weight of water; and a and n are van Genuchten (1980) SWCC fitting parameters shown in Eq. (7).

In Eq. (8), $Z = \gamma_w z/a$ where z is the distance between the bottom of the TC and the groundwater level so the TC depth is equal to (Z_o–Z). The parameter G in Eq. (8) represents the deformability of the soil and is equal to $[(1-2\mu/\mu)(\gamma_w/\gamma)]$ where μ is Poisson's ratio (taken to be 0.3 in this study), and γ is the total soil unit weight (which is 21.2 kN/m^3 in this study), resulting in G equal to 0.6 for the current study. For most soils, G ranges between 0.4 and 1.5, in which the larger values of G indicate relatively deformable or plastic materials (Lu and Likos 2004). Eq. (8) gives the steady-state estimate of the desiccation TC depth that assumes the embankment has sufficient time to develop the full steady-state depth, which is difficult in recently constructed embankments that experience rainfall, as in this case. The van Genuchten (1980) SWCC curve fitting parameters are used to estimate the desiccation TC depth from the embankment surface to perform the unsaturated inverse stability analysis of the embankment failure described subsequently.

Fig. 2 shows the sensitivity of the steady-state desiccation TC depth to the SWCC parameters a and n as well as to the deformability factor G. A maximum depth of the desiccation TC could be about 3.5 m for a value of G of 1.5 and $n = 1.1$, which does not change significantly with the value of a. Within the selected range of a and n van Genuchten (1980) SWCC fitting parameters, the impact of the two parameters on the depth of the desiccation TC is only 0.5–1.0 m. In future design projects, a sensitivity graph similar to Fig. 2 can be developed to estimate the range of desiccation TC depth to be modeled in the stability analysis for a range of the SWCC parameters that are properly selected for the type of compacted embankment material in question. In general, for a given combination of the SWCC parameters of a and n, a higher value of G will increase the desiccation TC depth and thus reduce the unsaturated shear strength of the compacted fill and resulting factor of safety.

Using Eq. (8), the steady-state depth of the desiccation TC for the compacted embankment is estimated to be 2.0 m (6.6 ft) based on van Genuchten (1980) fitting parameters of a and n equal to 47 kPa and 1.5, respectively, and a deformability factor G of 0.6. The groundwater level is located at a depth of $z_o = 6$ m from the embankment crest. However, field observations by the second author do not support a 2.0 m (6.6 ft) deep desiccation TC because the embankment had only been under construction for about 45 days, so a desiccation TC depth of 2.0 m (6.6 ft) is not feasible. Fill material kept being placed and photos in October 2007, see Fig. 3, show a much shallower TC than 2.0 m (6.6 ft) deep.

Fig. 3. (a) Overview of top of compacted embankment in vicinity of slope failure prior to failure; and (b) close-up of scarp that developed on embankment crest after slope movement.

A TC depth of about 0.15–0.30 m (0.5–1.0 ft) is more realistic. Therefore, Eq. (8) should not be used in the situation where the desiccation TC is still developing, however, in situations where an unsaturated clayey embankment has been in service for a long period, Eq. (8) could be applicable to estimate the steady-state desiccation TC depth if rainfall is infrequent.

Peron et al. (2009) indicated that desiccation cracking initiates close to the onset of desaturation or when the matric suction is close to the AEV. Yesiller et al. (2000) also described laboratory desiccation cracking of compacted clay specimens in terms of the surficial dimensions of the TCs when the specimens were subjected to cycles of drying and wetting using fans and a rain simulator, respectively. One of the specimens is close in plasticity to the compacted embankment fill material with a liquid limit $(LL) = 29$ and $PI = 13$ (Table 4). This specimen showed a maximum area of cracking under drying of 40–200 h after the application of the drying condition. Yesiller et al. (2000) found that after the first drying/wetting cycle, the material becomes weaker in resisting cracking or tensile stresses, and the area of desiccation cracking increases significantly. Although timing of tension cracking is not the focus of the paper, the first surface TC in the embankment appeared a few days after a 33°C (91°F) temperature was recorded in the area followed by a rain event (drying/wetting cycle). This suggests some desiccation cracking could have been present on the surface of the compacted embankment prior to slope movement so a shallow desiccation TC should be added to the depth of strain incompatibility cracking discussed subsequently.

Yesiller et al. (2000) did not study the cracking depth because the specimens were relatively thin with a thickness of 170 mm (6.7 in.) and had a homogenous matric suction. Eq. (8) provides a steady-state estimate of desiccation TC depth with the assumption of hydrostatic suction distribution within the unsaturated zone. The effect of climatic conditions on the change of suction distribution and, hence, TC depth with time needs further investigation.

In summary, Eq. (8) appears to overestimate the depth of a desiccation TC for typical unsaturated embankments during construction because steady-state conditions do not have time to develop and precipitation events can occur. Therefore, using the desiccation TC depth from Eq. (8) yields too low of a FS because it eliminates too much shear strength from the compacted embankment to the stability analysis.

Strain Incompatibility TC Depth

A TC is required to account for strain incompatibility between the soft foundation soils and the overlying stiff and brittle compacted fine-grained embankment and is also required for the following unsaturated stability analysis. This is due to lateral deformation of the soft foundation soils parallel and away from the embankment centerline under the weight of the compacted fill in which the softer foundation peak strength is mobilized at a higher shear displacement or strain than the stiffer and brittle overlying compacted embankment. During this lateral deformation, the peak strength of the stiff embankment material is mobilized locally resulting in a TC that will start at the embankment/foundation soil interface and propagate upward through the embankment (Chirapuntu and Duncan 1976). This case is different from the classical case in which the strength of the embankment and foundation soils are mobilized simultaneously resulting in tension stresses and cracking at the top of the embankment.

Eq. (9), developed by Lu and Likos (2004), extends Rankine's active earth pressure theory by incorporating matric suction

Table 5. Height of strain incompatibility tension crack using unsaturated soil properties and Eqs. (1) and (10)

Tension crack location in compacted embankment	Elevation from top of sand blanket (Fig. 1) (m)	$(u_a - u_w)$ (kPa)	$\theta(\mathrm{m}^3/\mathrm{m}^3)$ Eq. (4)	$\frac{\theta-\theta_r}{\theta_s-\theta_r}$ Eq. (6)	Total stress cohesion, c or Su (kPa)	Total stress friction angle, ϕ (degrees)	Effective stress cohesion, c' (kPa)	Effective stress friction angle, ϕ' (degrees)	H_{crack} (m) using Eq. (1)	z_{Si} (m) using Eq. (9)
Bottom of embankment	300.2	29.4	0.39	0.9	N/A	N/A	0	33	0.0	0.9
					N/A	N/A	11.0	33	1.6	2.8
					N/A	N/A	14.4	33	2.5	3.4
					71.8	0	N/A	N/A	6.7	6.7

pressures to estimate the depth of the strain incompatibility TC as shown in the following expression:

$$z_{si} = \frac{2c' + \left[\frac{\theta - \theta_r}{\theta_s - \theta_r}(u_a - u_w)\right](1 - k_a)/\sqrt{k_a}}{\gamma\sqrt{k_a}} \tag{9}$$

where k_a = coefficient of Rankine active earth pressure given by $k_a = \tan^2[45° - (\phi'/2)]$. This height is used as an estimate of the strain incompatibility height, Z_{si}, in an unsaturated embankment. With no matric suction pressures, Eq. (9) simplifies to the TC depth expression presented in Eq. (1).

Eq. (9) calculates the height of TC due to strain incompatibility based on the unsaturated tensile strength of the compacted fill, but it does not include the effect of the stiffness difference between the compacted embankment and soft foundation soils as presented in the Chirapuntu and Duncan (1976) method. For comparison purposes, Table 5 shows the height of the strain incompatibility crack calculated using Eqs. (1) and (9) at the bottom of the embankment fill and above the sand blanket. The height of the strain incompatibility TC in the fine-grained embankment varies from 0.9 to 3.4 m (Table 5) using the range of effective stress cohesion (0–14.4 kPa) and friction angle (ϕ') of 33° obtained from an inverse analysis of the failure by Stark et al. (2018). If an undrained shear strength of 71.8 kPa is used for the compacted embankment, both equations yield the same TC length of 6.7 m, which exceeds the height of the embankment at failure.

In this case history, a 0.9 m (3 ft) thick sand blanket (Fig. 1) was installed on the ground surface to promote drainage from the PVDs so the strain incompatibility crack is applied from the top of the sand blanket. This is different than the traditional configuration where a stiff compacted embankment is placed directly on the surface of the soft foundation soils, as shown in Chirapuntu and Duncan (1976). Because the 0.9 m (3 ft) thick sand blanket is comprised of cohesionless soil, it will not maintain an open TC like the unsaturated and fine-grained embankment material. For example, Fig. 4 shows open TCs on the surface of the compacted embankment prior to failure at an embankment height of only 4.0 m (13 ft).

However, the shear strength of the sand blanket was reduced using the procedure in Chirapuntu and Duncan (1976) to account for progressive failure and the strain incompatibility between the compacted embankment system and soft foundation soils, which would induce tensile stresses in the sand blanket. Strain incompatibility exists because the embankment and foundation soils exhibit brittle stress-strain and ductile stress-strain behaviors, respectively. In particular, the soft foundation clays do not exhibit a large post-peak strength loss like the compacted embankment so a reduction factor was not applied to the foundation soils. While a TC would develop in the compacted clayey embankment, a reduction factor, R_E, of 0.77 was used for the sand blanket shear strength to reflect a reduced strength due to the development of tensile stresses in the sand blanket caused by TC development and/or lateral spreading. This reduction factor was estimated using the average shear strength of the foundation soils, $S_{F,ave}$, and compacted embankment, $S_{E,ave}$, as calculated

$$S_{F,ave} = \frac{\Sigma S_{u,i} \times d_i}{d_{total}} = \frac{(36\ \text{kPa} \times 2.4\ \text{m}) + (12\ \text{kPa} \times 3.14\ \text{m}) + (9.6\ \text{kPa} \times 3.0\ \text{m}) + (48\ \text{kPa} \times 1.2\ \text{m})}{(2.4\ \text{m} + 3.1\ \text{m} + 3.0\ \text{m} + 1.2\ \text{m})} = 21.7\ \text{kPa} \tag{10}$$

$$\begin{aligned} S_{E,ave} &= \frac{\Sigma[c'_i + \sigma'_i \times \tan(\phi'_i)] \times d_i}{d_{total}} \\ &= \frac{\left[11.0\ \text{kPa} + \left(21.2\frac{\text{kN}}{\text{m}^3} \times 1.55\ \text{m} \times \tan(33^0)\right)\right] \times 3.1\ \text{m} + \left[0\ \text{kPa} + \left(\left\langle\left(21.2\frac{\text{kN}}{\text{m}^3} \times 3.1\ \text{m} + 18.6\frac{\text{kN}}{\text{m}^3} \times 0.45\ \text{m}\right)\right\rangle \times \tan(33^0)\right)\right] \times 3.1\ \text{m}}{(3.1\ \text{m} + 0.9\ \text{m})} \\ &= 35.8\ \text{kPa} \end{aligned} \tag{11}$$

The ratio of the average embankment strength to the average foundation strength is 35.8/21.7 kPa, or about 1.6. The value of R_E equals about 0.77 for a ratio of embankment to foundation soil strength of 1.6 from Fig. 4.11 of Chirapuntu and Duncan (1976). Applying a reduction factor of 0.77 to the effective stress friction angle of 33° yields an effective stress friction angle for the sand blanket of 26° ($\tan^{-1}$ [tan(33°) × 0.77]), which was used in the stability analysis to model the sand blanket with a $c' = 0$.

Based on the preceding discussion, summing the estimated desiccation TC depth of 0.15–0.3 m (0.5–1.0 ft), and the strain incompatibility TC height of 0.9–3.4 m (2.9–11.2 ft) yields a total TC height in the fine-grained embankment of between 1.05 and 3.70 m (3.4–12.2 ft). The upper bound depth of 3.7 m is greater than the height of the compacted fine-grained embankment of 3.1 m (10 ft) at failure where the TC is expected to occur. TCs started developing along the crest of the embankment after a total embankment height of only 2.4 m (8 ft), which includes the sand blanket of 0.9 m (3 ft) and the fine-grained compacted embankment of 1.5 m (5 ft) (Fig. 4), and failure occurred when the fine-grained embankment height was 3.1 m (10 ft). Both heights are encompassed by the total TC range between 1.05 and 3.70 m (3.4–12.2 ft) so the embankment mobilized little strength at the time of failure. In summary, utilizing a TC that is a summation of the desiccation TC depth and strain incompatibility TC height is in agreement with field observations. A total TC height of 3.1 m (10 ft), which covers the full fine-grained embankment height at the time of failure, is used in the following inverse stability analysis to investigate the mobilized unsaturated shear strength of the compacted embankment.

Unsaturated Stability Analysis for Connector Ramp

For the unsaturated slope stability analysis, the applied TC of 3.1 m (10.0 ft) is the sum of the desiccation TC of 0.3 m (1.0 ft) starting at the top of the embankment, and the strain incompatibility TC

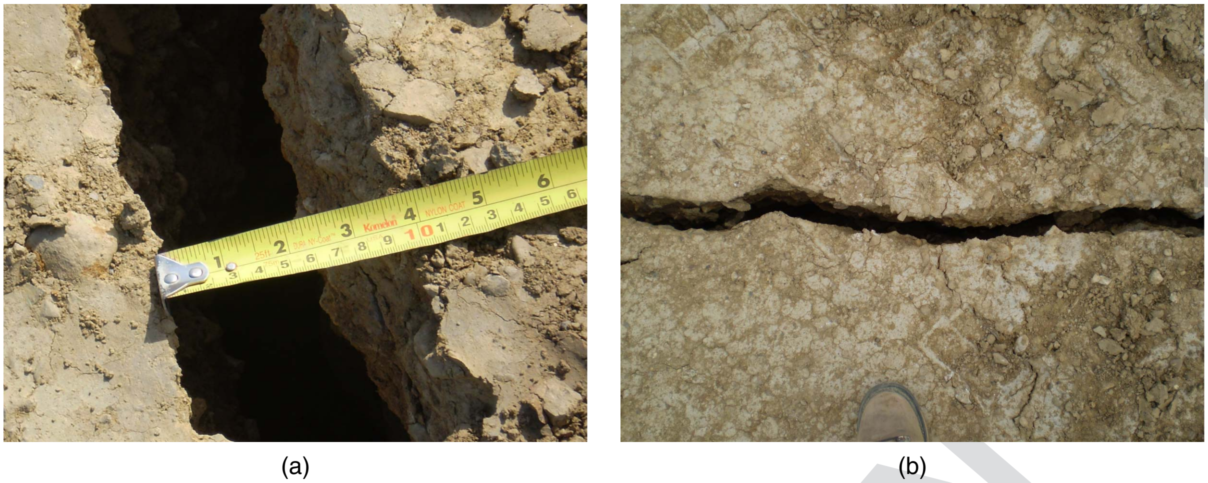

Fig. 4. Open tension cracks on top of compacted embankment in vicinity of slope failure at an embankment height of 2.4 m (8 ft).

[Eq. (9)] starting at the bottom of the fine-grained embankment 2.8 m (9.0 ft) corresponding to an effective stress cohesion, c', of 11.0 kPa, and an effective stress friction angle, ϕ', of 33°. An inverse analysis was used to estimate the c' value of 11.0 kPa using ϕ' of 33° and to achieve a FS of 0.99. Because unsaturated strength is accounted for, this value is reduced from 14.4 kPa in the saturated case (Stark et al. 2018). The inverse slope stability analysis was performed using the SLOPE/W software (Geo-Slope 2012) and the Morgenstern and Price (1965) stability method. The matric suction was accounted for in the compacted fill material by assigning a volumetric moisture content function based on the van Genuchten (1980) model. The SLOPE/W software uses the $\tan \phi^b$ term in Eqs. (2) and (5) from Vanapalli et al. (1996) to calculate the matric suction contribution to the shear strength of the unsaturated compacted fill material. A TC length of 3.1 m (10 ft) was introduced using the tension crack feature in SLOPE/W from the top of the sand blanket to the top of the compacted embankment.

To account for the progressive failure in the sand blanket, the shear strength of the sand blanket was reduced ($\phi' = 26°$) using the procedure in Chirapuntu and Duncan (1976) to account for the strain incompatibility between the soft foundation soils and compacted embankment as previously described.

By applying search increments for the entry and exit ranges at the embankment surface and slope toe, respectively, the observed failure surface (Fig. 1) was modeled in the inverse stability analysis. This analysis models the compacted fill with an effective stress cohesion and friction angle of 11.0 kPa and 33°, respectively, instead of an undrained shear strength of 71.8 kPa (1,500 psf). In this case, and because the TC depth essentially encompasses the full height of the embankment at the time of failure, the unsaturated shear strength did not contribute significantly to the shear resistance mobilized along the failure surface. Fig. 5 shows that the resulting FS is 0.99, which is in agreement with the onset of failure being observed at an embankment height of only 4.0 m (13 ft).

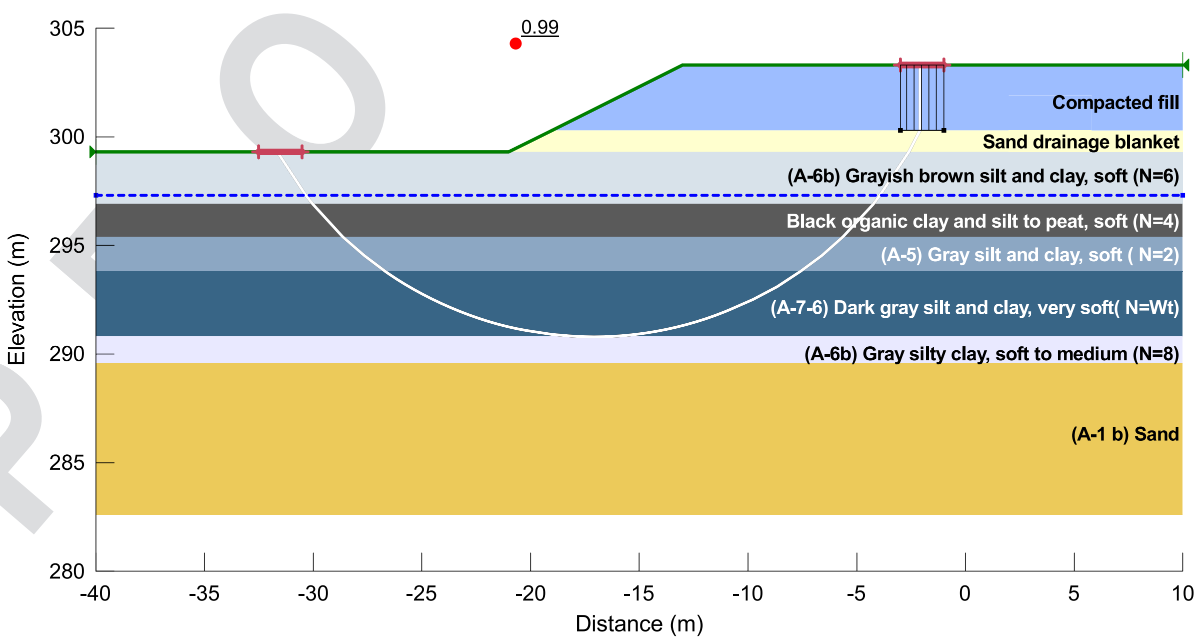

Fig. 5. Unsaturated inverse analysis of connector embankment using an effective stress cohesion of 11.0 kPa, friction angle of 33°, and matric suction for the compacted embankment fill.

In addition, the failure surface that yields a FS of 0.99 is in agreement with the observed failure surface shown in Fig. 1.

Unsaturated Shear Strength of Embankment Fill

Fortunately or unfortunately, the TC due to primarily the soft foundation soils and some surficial desiccation resulted in the crack depth exceeding the height of the embankment at failure. As a result, it was not necessary to estimate the unsaturated shear strength of the embankment fill, which can be a challenge. Estimating the unsaturated shear strength of embankment fill for other projects will be important for design and possibly inverse analyses. The unsaturated methodology used to estimate compacted embankment shear strength for this case is illustrated in Appendix S1 and provides a worked example of this methodology. This unsaturated shear strength estimate is applicable where the embankment is not cracked the full height due to desiccation and/or strain incompatibility, as in this case history. Using this method, the unsaturated embankment can be modeled with unsaturated shear strength to investigate the range of FS with suction pressures.

Chirapuntu and Duncan (1976) Strain Incompatibility Example

To further verify the use and practical significance of unsaturated soil mechanics to model a compacted embankment over soft foundation soils, the method previously described was applied to the example in Chirapuntu and Duncan (1976) to illustrate how unsaturated soil mechanics can be incorporated into a stability analysis when the TC does not extend the full height of the embankment so the embankment has to be modeled using unsaturated soil strength parameters, which differs from the preceding case history. This example also shows that when properly considered, the contribution of suction in unsaturated slopes will not necessarily result in a higher FS and the difficulties obtaining the analysis input parameters. This example is presented in Appendix S2 but may be of use to practitioners for cases where the TC does not extend the full height of the embankment.

Summary and Recommendations

This paper describes the use of unsaturated soil mechanics to investigate the failure of an interstate connecting-ramp embankment during construction. Based on the unsaturated stability analysis presented, the following recommendations are made for evaluating the stability of unsaturated, stiff compacted embankments over soft foundation soils:

- Incorporating the contribution of matric suction into a stability analysis of an unsaturated compacted embankment leads to a more representative stress state at which the embankment exists after compaction than assuming an undrained stability analysis that uses an undrained shear strength to model the embankment.
- Both desiccation and strain incompatibility TCs should be considered when analyzing an unsaturated embankment. The desiccation TC is associated with shrinkage of the fine-grained embankment fill near the top of the embankment and low shear resistance in tension, which also occurs along the embankment slopes. Reviewing recorded climatic parameters in the embankment area is helpful to evaluate the extent of desiccation cracking because steady-state desiccation cracking probably does not have sufficient time to develop in most areas. The strain incompatibility TC is due to lateral extension of the soft foundation soils in which the foundation peak strength is mobilized at a higher shear displacement or strain than the stiffer and brittle compacted embankment.
- The inverse analysis presented herein does not account for changes in shear-induced pore water pressures, if any, along the failure surface within the unsaturated embankment. However, in this case, both the desiccation and strain incompatibility TCs resulted in a TC over the full height of the embankment fill so the effect of shear-induced pore water pressures in the embankment was not needed for this analysis.

Data Availability Statement

Some or all data, models, or code that support the findings of this study are available from the corresponding author upon reasonable request.

Acknowledgments

The contents and views in this paper are those of the individual authors and do not necessarily reflect those of any of the represented corporations, contractors, agencies, consultants, organizations, and/or contributors including ODOT and the US Army Corps of Engineers. The second author appreciates the financial support of the National Science Foundation (NSF Award CMMI-1562010). The contents and views in this paper are those of the individual authors and do not necessarily reflect those of the National Science Foundation.

Supplemental Materials

Appendixes S1 and S2 are available online in the ASCE Library (www.ascelibrary.org).

References

ASTM. 2009. *Standard practice for description and identification of soils (visual manual procedure)*. ASTM D2488. West Conshohocken, PA: ASTM.

ASTM. 2014. *Standard test method for moisture, ash, and organic matter of peat and other organic soils*. ASTM D2974. West Conshohocken, PA: ASTM.

ASTM. 2017. *Standard practice for classification of soils for engineering purposes (unified soil classification system)*. ASTM D2487. West Conshohocken, PA: ASTM.

Aubertin, M., M. Mbonimpaa, B. Bussièreb, and R. P. Chapuis. 2003. "A physically-based model to predict the water retention curve from basic geotechnical properties." *Can. Geotech. J.* 40 (6): 1104–1122. https://doi.org/10.1139/t03-054.

Benson, C., I. Chiang, T. Chalermyanont, and A. Sawangsuriya. 2014. "Estimating van Genuchten parameters α and n for clean sands from particle size distribution data." In *Proc., Soil Behavior Fundamentals to Innovations in Geotechnical Engineering*, 410–427.

Brooks, R. H., and A. T. Corey. 1964. *Hydraulic properties of porous media: Hydrology papers 3*, 27. Fort Collins, CO: Colorado State Univ.

Chirapuntu, S., and J. M. Duncan. 1976. *The role of fill strength in the stability of embankments on soft clay foundations*. Contract Rep. No. S-76-6. Berkeley, CA: US Army Engineer, Waterways Experiment Station, Univ. of California at Berkeley.

Ellithy, G. 2017. *A spreadsheet for estimating soil water characteristic curves (SWCC)*. ERDC/GSL TN-17-1. Vicksburg, MS: US Army Engineer Research and Development Center.

Ellithy, G., F. Vahedifard, and X. Rivera-Hernandez. 2017. "Accuracy assessment of predictive SWCC models for estimating the van Genuchten model parameters." In *Proc., PanAm-Unsat Conf.* Reston, VA: ASCE.

Fredlund, D. G. 2002. "Use of the soil-water characteristic curve in the implementation of unsaturated soil mechanics." In *Proc., 3rd Int. Conf. on Unsaturated Soils*, 887–902. Recife, Brazil. [31]

Fredlund, D. G., N. R. Morgenstern, and R. A. Widger. 1977. "Stress state variables for unsaturated soils." *J. Geotech. Div.* 103 (5): 447–466. [32]

Fredlund, D. G., N. R. Morgenstern, and R. A. Widger. 1978. "The shear strength of unsaturated soils." *Can. Geotech. J.* 15 (3): 313–321. https://doi.org/10.1139/t78-029.

Fredlund, D. G., and J. Rahardjo. 1993. *Soil mechanics for unsaturated soils*. New York: Wiley.

Fredlund, D. G., J. Rahardjo, and M. D. Fredlund. 2012. *Unsaturated soil mechanics in engineering practice*. New York: Wiley.

Fredlund, D. G., and S. K. Vanapalli. 2002. "Shear strength of unsaturated soils." In *Agronomy soil testing manual*, 329–361. Madison, WI: Agronomy Society of America.

Fredlund, D. G., and A. Xing. 1994. "Equations for the soil-water characteristic curve." *Can. Geotech. J.* 31 (4): 521–532. https://doi.org/10.1139/t94-061.

Gardner, W. R. 1958. "Some steady state solutions of unsaturated moisture flow equations with applications to evaporation from a water table." *Soil Sci.* 85 (4): 228–232. https://doi.org/10.1097/00010694-195804000-00006.

Garven, E. A., and S. K. Vanapalli. 2006. "Evaluation of empirical procedures for predicting the shear strength of unsaturated soils." In *Proc., 4th Int. Conf. of Unsaturated Soils*, 2570–2581. [33]

Gasmo, J. M., H. Rahardjo, and E. C. Leong. 2000. "Infiltration effects on stability of a residual soil slopes." *Comput. Geotech.* 26 (2): 145–165. https://doi.org/10.1016/S0266-352X(99)00035-X.

Geo-Slope. 2012. *Slope/W software users guide*. Calgary, AB: GeoSlope.

Khalili, N., and M. H. Khabbaz. 1998. "Unique relationship for χ for the determination of the determination of the shear strength of unsaturated soils." *Géotechnique* 48 (5): 681–687. https://doi.org/10.1680/geot.1998.48.5.681. [34]

Lau, J. T. 1987. "Desiccation cracking of soils." M.S. thesis, Univ. of Saskatchewan. [35]

Lu, N., and W. Likos. 2004. *Unsaturated soil mechanics*. New York: Wiley.

Michalowski, R. L. 2014. "Stability assessment of slopes with cracks using limit analysis." *Can. Geotech. J.* 50 (10): 1011–1021. https://doi.org/10.1139/cgj-2012-0448.

Morgenstern, N. R., and V. E. Price. 1965. "The analysis of the stability of general slip surface." *Géotechnique* 15 (1): 79–93. https://doi.org/10.1680/geot.1965.15.1.79.

Ng, C. W., and Q. Shi. 1998. "A numerical investigation of the stability of unsaturated soil slopes subjected to transient seepage." *Comput. Geotech.* 22 (1): 1–28. https://doi.org/10.1016/S0266-352X(97)00036-0.

ODOT (Ohio Department of Transportation). 2010. *Shear strength of proposed embankments*. Geotechnical Bulletin No. 6. Columbus, OH: Division of Production Management Office of Geotechnical Engineering, ODOT.

Oh, S., and N. Lu. 2015. "Slope stability analysis under unsaturated conditions: Case studies of rainfall-induced failure of cut slopes." *Eng. Geol.* 184 (Jan): 96–103. https://doi.org/10.1016/j.enggeo.2014.11.007.

Oh, W. T., and S. K. Vanapalli. 2010. "Influence of rain infilteration on the stability of compacted soil slopes." *Comput. Geotech.* 37 (5): 649–657. https://doi.org/10.1016/j.compgeo.2010.04.003.

Peck, R. B., W. E. Hanson, and T. H. Thornburn. 1974. *Foundation engineering practice*. 3rd ed., 514. New York: Wiley.

Peron, H., L. Laloui, T. Hueckel, and L. B. Hu. 2009. "Desiccation cracking of soils." *Eur. J. Environ. Civ. Eng.* 13 (7–8): 869–888. https://doi.org/10.1080/19648189.2009.9693159.

Stark, T. D., and J. M. Duncan. 1991. "Mechanisms of strength loss in stiff clays." *J. Geotech. Eng.* 117 (1): 139–154. https://doi.org/10.1061/(ASCE)0733-9410(1991)117:1(139).

Stark, T. D., and M. Hussain. 2013. "Drained shear strength correlations for slope stability analyses." *J. Geotech. Geoenviron. Eng.* 139 (6): 853–862. https://doi.org/10.1061/(ASCE)GT.1943-5606.0000824. [36]

Stark, T. D., R. D. Sisk, and P. J. Ricciardi. 2018. "Case study: Stability and vertical drain analyses for embankment failure on soft soils." *J. Geotech. Geoenviron. Eng.* 144 (2): 05017007. https://doi.org/10.1061/(ASCE)GT.1943-5606.0001786.

van Genuchten, M. T. 1980. "A closed-form equation for predicting the hydraulic conductivity of unsaturated soils." *Soil Sci. Soc. Am. J.* 44 (5): 892–898. https://doi.org/10.2136/sssaj1980.03615995004400050002x.

Vanapalli, S. K., D. E. Fredlund, and D. E. Pufahl. 1996. "Model for the prediction of shear strength with respect to soil suction." *Can. Geotech. J.* 33 (3): 379–392. https://doi.org/10.1139/t96-060.

Vanapalli, S. K., and D. G. Fredlund. 2000. "Comparison of empirical procedures to predict the shear strength of unsaturated soils using the soil-water characteristic curve." *Adv. Unsaturated Geotech.* 99: 195–209. [37] [38]

Vanapalli, S. K., D. E. Pufahl, D. G. Fredlund, and A. W. Clifton. 1999. "Interpretation of the shear strength of unsaturated soils in undrained loading conditions." In *Proc., 52nd Canadian Geotechnical Conf.*, 643–650. Regina, SK. [39]

Yesiller, N., C. J. Miller, G. Inci, and K. Yaldo. 2000. "Desiccation and cracking behavior of three compacted landfill liner soils." *Eng. Geol.* 57 (1–2): 105–121. https://doi.org/10.1016/S0013-7952(00)00022-3.

Zapata, C. E., W. N. Houston, S. L. Houston, and K. D. Walsh. 2000. "Soil-water characteristic curve variability." In *Proc., ASCE Geotechnical Special Publication 99*, 84–124. Reston, VA: ASCE.

Queries

1. Please check the hierarchy of section heading levels.

2. ASCE Open Access: Authors may choose to publish their papers through ASCE Open Access, making the paper freely available to all readers via the ASCE Library website. ASCE Open Access papers will be published under the Creative Commons-Attribution Only (CC-BY) License. The fee for this service is $2000, and must be paid prior to publication. If you indicate Yes, you will receive a follow-up message with payment instructions. If you indicate No, your paper will be published in the typical subscribed-access section of the Journal.

3. Please check all figures, figure citations, and figure captions to ensure they match and are in the correct order.

4. Any and all acronyms/abbreviations included in any figure must either have been previously defined within the text, or be defined in a note immediately following the figure caption (e.g., . . .inferred failure surface (dashed line). Su = definition; A = definition.)

5. The format of Table 1 has been altered. Please review.

6. Please review the deletion of the word "and" in the first column of Table 1.

7. All acronyms/abbreviations must be defined upon first use. Please fully define USCS, MH, and CL in Table 1, either in the body of the table or in a note to the table (e.g., Note: USCS = definition; MH = definition; and CL = definition)

8. ASCE style for math is to set all mathematical variables in italic font. Please check all math variables throughout the paper, both in equations and text, to ensure all conform to ASCE style.

9. All lowercase Greek letters have been set to italics in equations and text, per ASCE requirements. Please verify that this is okay.

10. All acronyms/abbreviations must be defined upon first use. Please fully define FS.

11. All specifically cited standards must include a citation and Reference list entry. Please insert an appropriate citation and provide all information for the ODOT specifications and they will be added to the References.

12. Per ASCE guidelines, there must be at least two subheadings under a heading. Both "Undrained Strain Incompatibilty" and "Use of SWCC to Estimate tanϕ^b" are the only Heading 2 subheadings under their respective Heading 1 headings. Please rework the heading levels to comply with ASCE style.

13. Per ASCE style, asterisks in equations have been changed to multiplication signs (×) throughout. Please review and verify that they have been correctly applied.

14. Please confirm that the change from a superscript lowercase "o" to the proper degree symbol is correct for Eq. (1).

15. Per ASCE style, the use of quotation marks for emphasis purposes is not allowed. If emphasis is required, please place the word or phrase in italics. As such, quotation marks have been removed from "tricking." Please review and determine if italics are needed instead.

16. All uppercase Greek letters have been set to roman (not italic) in equations and text, per ASCE requirements. Please verify that this is okay.

17. Per ASCE style, the use of quotation marks for emphasis purposes is not allowed. If emphasis is required, please place the word or phrase in italics. As such, quotation marks have been removed from "wetting." Please review and determine if italics are needed instead.

18. For Eq. (7) variable explanation, there are three parameters listed (a, n, and m), but four parameter definitions. Please review this explanation and change it to reflect the correct number of parameters and parameter definitions (the numbers should match).

19. Please make sure that all values that need a unit of measure include a unit of measure.

20. All acronyms/abbreviations must be defined upon first use. Please verify that LL has been properly defined.

21. Please review the addition of the word “and” in the sentence that begins “A TC is required. . .” If it is incorrect, please rewrite the sentence to avoid reader confusion.

22. All acronyms/abbreviations must be defined upon first use. Please fully define PVD.

23. Please provide version number for SLOPE/W software.

24. Per ASCE style, the use of quotation marks for emphasis purposes is not allowed. If emphasis is required, please place the word or phrase in italics. As such, quotation marks have been removed from “tension crack.” Please review and determine if italics are needed instead.

25. Per ASCE style, the use of quotation marks for emphasis purposes is not allowed. If emphasis is required, please place the word or phrase in italics. As such, quotation marks have been removed from “search increments. Please review and determine if italics are needed instead.

26. Please review the sentence that begins “This example also. . .”

27. This reference ASTM (2009) is not mentioned anywhere in the text. ASCE style requires that entries in the References list must be cited at least once within the paper. Please indicate a place in the text, tables, or figures where we may insert a citation or indicate if the entry should be deleted from the References list.

28. This reference ASTM (2014) is not mentioned anywhere in the text. ASCE style requires that entries in the References list must be cited at least once within the paper. Please indicate a place in the text, tables, or figures where we may insert a citation or indicate if the entry should be deleted from the References list.

29. This reference ASTM (2017) is not mentioned anywhere in the text. ASCE style requires that entries in the References list must be cited at least once within the paper. Please indicate a place in the text, tables, or figures where we may insert a citation or indicate if the entry should be deleted from the References list.

30. Please provide the publisher or sponsor name and location (not the conference location) for Benson et al. (2014).

31. Please provide the publisher or sponsor name and location (not the conference location) for Fredlund (2002).

32. This query was generated by an automatic reference checking system. This reference could not be located in the databases used by the system. While the reference may be correct, we ask that you check it so we can provide as many links to the referenced articles as possible.

33. Please provide the publisher or sponsor name and location (not the conference location) for Garven and Vanapalli (2006).

34. This reference Khalili and Khabbaz (1998) is not mentioned anywhere in the text. ASCE style requires that entries in the References list must be cited at least once within the paper. Please indicate a place in the text, tables, or figures where we may insert a citation or indicate if the entry should be deleted from the References list.

35. Please provide department name for Lau (1987).

36. This reference Stark and Hussain (2013) is not mentioned anywhere in the text. ASCE style requires that entries in the References list must be cited at least once within the paper. Please indicate a place in the text, tables, or figures where we may insert a citation or indicate if the entry should be deleted from the References list.

37. Please provide issue number for Vanapalli and Fredlund (2000).

38. This query was generated by an automatic reference checking system. This reference could not be located in the databases used by the system. While the reference may be correct, we ask that you check it so we can provide as many links to the referenced articles as possible.

39. Please provide the publisher or sponsor name and location (not the conference location) for Vanapalli et al. (1999).